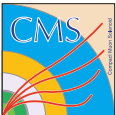




III. Physikalisches
Institut A

RWTHAACHEN
UNIVERSITY



Search for heavy resonances in two-particle final states with leptons, jets and photons at CMS

Andreas Güth
for the CMS Collaboration

III. Physikalisches Institut A, RWTH Aachen

SPONSORED BY THE



Federal Ministry
of Education
and Research

Particles and Nuclei International Conference 2014
Hamburg

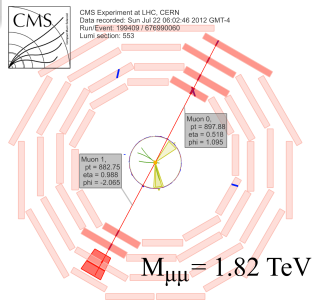
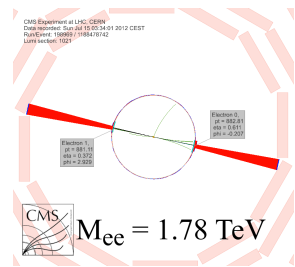
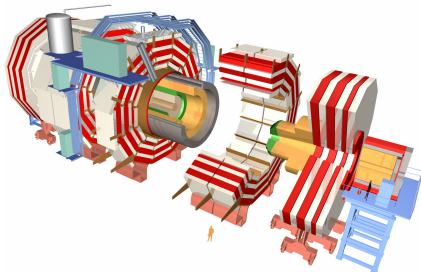
August 28th 2014

DFG

Introduction

Outline

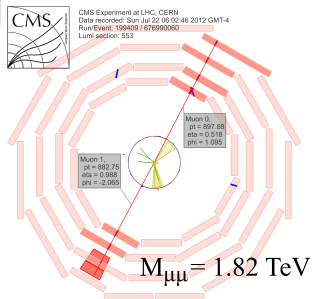
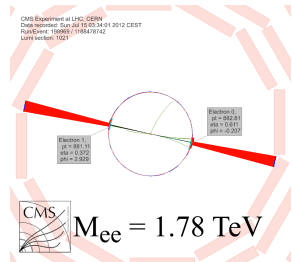
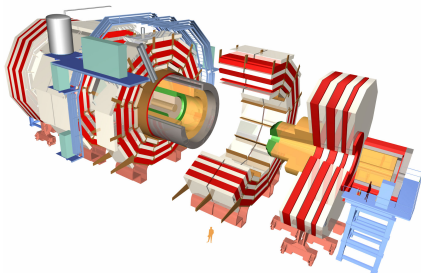
- CMS detector and performance
- Search for $\mu\mu$, ee resonances
- Search for jj resonances
- Search for γj resonances
- Projections for $Z' \rightarrow \mu\mu$, ee at $\sqrt{s} = 14$ TeV
- Conclusion



Introduction

Outline

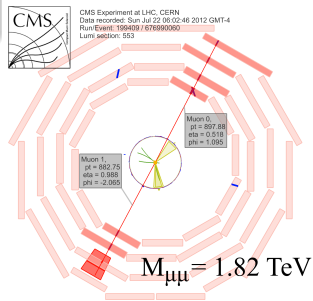
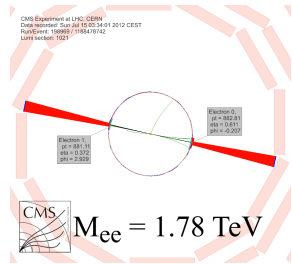
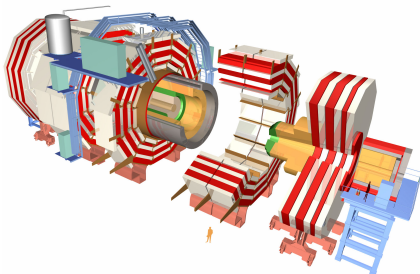
- CMS detector and performance
- Search for $\mu\mu, ee$ resonances
- Search for jj resonances
- Search for γj resonances
- Projections for $Z' \rightarrow \mu\mu, ee$ at $\sqrt{s} = 14$ TeV
- Conclusion



Introduction

Outline

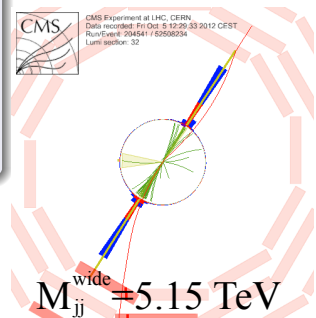
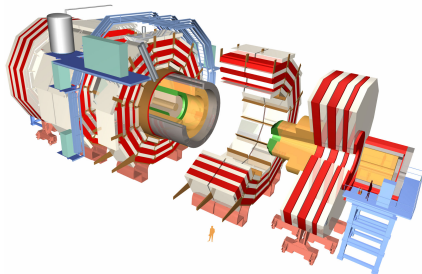
- CMS detector and performance
- Search for $\mu\mu, ee$ resonances
CMS-PAS-EXO-12-061
- Search for jj resonances
- Search for γj resonances
- Projections for $Z' \rightarrow \mu\mu, ee$ at $\sqrt{s} = 14$ TeV
- Conclusion



Introduction

Outline

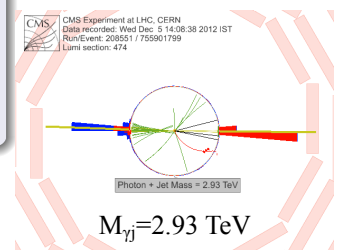
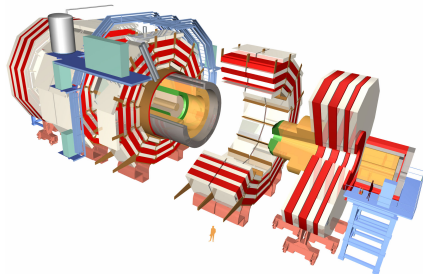
- CMS detector and performance
- Search for $\mu\mu$, ee resonances
- **Search for jj resonances**
[CMS-PAS-EXO-12-059](#) , [CMS-PAS-EXO-12-023](#)
- Search for γj resonances
- Projections for $Z' \rightarrow \mu\mu$, ee at $\sqrt{s} = 14$ TeV
- Conclusion



Introduction

Outline

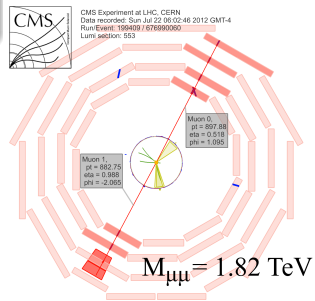
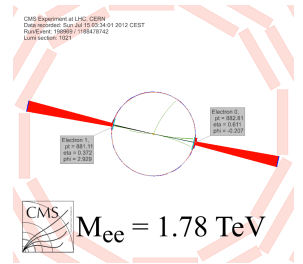
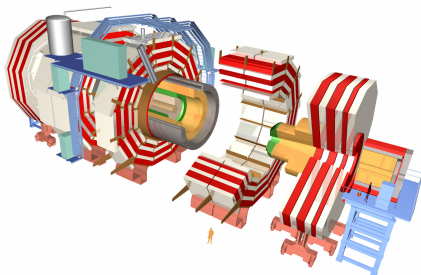
- CMS detector and performance
 - Search for $\mu\mu$, ee resonances
 - Search for jj resonances
 - **Search for γj resonances**
- CMS-PAS-EXO-13-003 , arXiv:1406.5171
- Projections for $Z' \rightarrow \mu\mu$, ee at $\sqrt{s} = 14$ TeV
 - Conclusion



Introduction

Outline

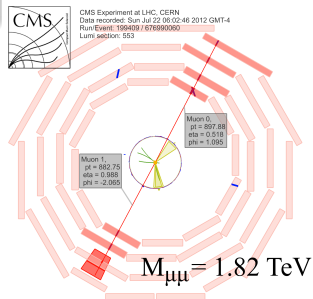
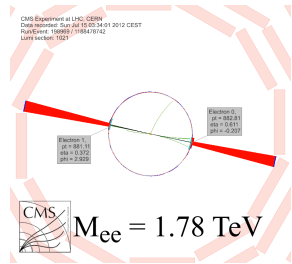
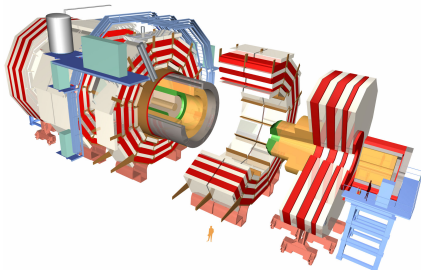
- CMS detector and performance
- Search for $\mu\mu$, ee resonances
- Search for jj resonances
- Search for γj resonances
- Projections for $Z' \rightarrow \mu\mu, ee$ at $\sqrt{s} = 14$ TeV
CMS-NOTE-2013-002 , arXiv:1307.7135
- Conclusion



Introduction

Outline

- CMS detector and performance
- Search for $\mu\mu$, ee resonances
- Search for jj resonances
- Search for γj resonances
- Projections for $Z' \rightarrow \mu\mu$, ee at $\sqrt{s} = 14$ TeV
- Conclusion



Introduction

Outline

- CMS detector and performance
- Search for $\mu\mu$, ee resonances
- Search for jj resonances
- Search for γj resonances
- Projections for $Z' \rightarrow \mu\mu$, ee at $\sqrt{s} = 14$ TeV
- Conclusion

For more results of searches for high-mass resonances at CMS see the results web pages from the **EXO** and **B2G** groups

<https://twiki.cern.ch/twiki/bin/view/CMSPublic/PhysicsResultsEXO>

<https://twiki.cern.ch/twiki/bin/view/CMSPublic/PhysicsResultsB2G>

CMS detector

Relative dilepton invariant mass resolution

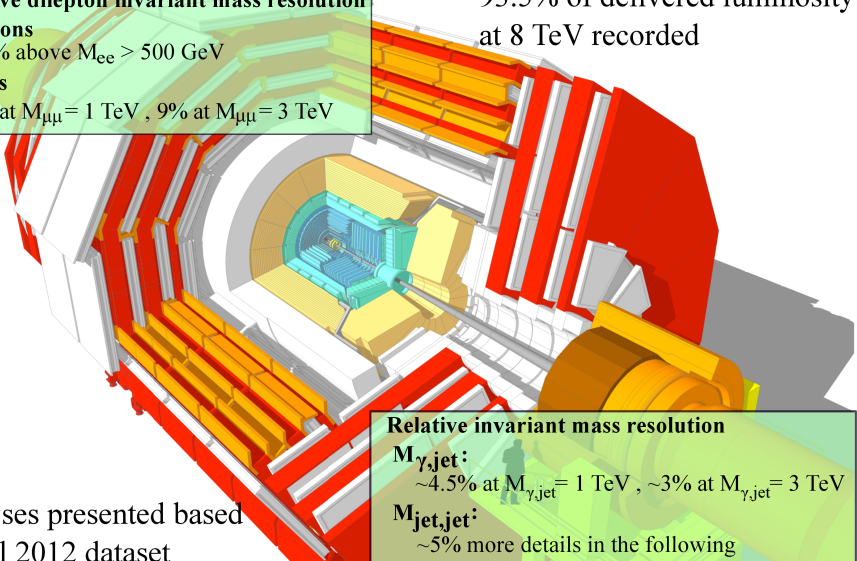
Electrons

1.5% above $M_{ee} > 500$ GeV

Muons

4% at $M_{\mu\mu} = 1$ TeV , 9% at $M_{\mu\mu} = 3$ TeV

93.5% of delivered luminosity
at 8 TeV recorded



Analyses presented based
on full 2012 dataset

Relative invariant mass resolution

$M_{\gamma,\text{jet}}$:

~4.5% at $M_{\gamma,\text{jet}} = 1$ TeV , ~3% at $M_{\gamma,\text{jet}} = 3$ TeV

$M_{\text{jet,jet}}$:

~5% more details in the following

Dilepton resonances - Signal models

CMS-PAS-EXO-12-061

Z' models considered in this talk

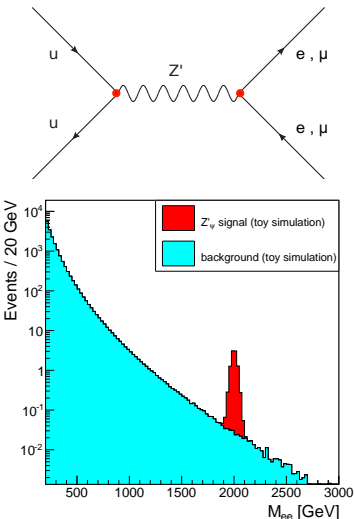
- Z'_{SSM} (Sequential Standard Model) with the same couplings to quarks and leptons as Z
- Z'_ψ from theories with E_6 GUT group
- Shape-based search for narrow resonance:
Reduction of model-dependent effects
(low-mass tails, Z'/Z interference)
- Further high-mass dilepton searches published by CMS:

RS graviton (spin-2 resonance)

Phys. Lett. B 720 (2013) 63

Large extra dimensions (non-resonant)

CMS-PAS-EXO-12-027 and CMS-PAS-EXO-12-031



Toy simulation of the invariant mass spectrum of dielectron events with a Z' signal at $M_{Z'} = 2$ TeV.

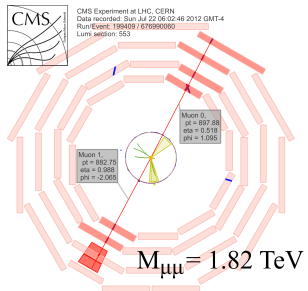
The event yield is normalized to 19.6 fb^{-1} at $\sqrt{s} = 8 \text{ TeV}$.

Dilepton resonances - Selection

Dimuon event selection

Single-muon trigger, $p_T^\mu > 40$ GeV, $|\eta^\mu| < 2.1$

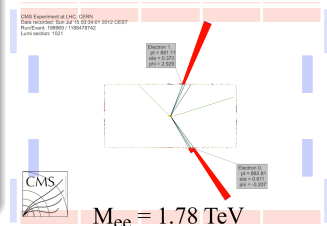
- Two muons with $p_T^\mu > 45$ GeV, $|\eta^\mu| < 2.4$
- Muons carry opposite electric charge



Dielectron event selection

Double-electron trigger, $E_T > 33$ GeV

- Two selected electrons with $E_T > 35$ GeV
- Analysis split into two channels with different background compositions
 - Both electrons in barrel $|\eta| < 1.422$
 - One electron in barrel and one in endcap $1.560 < |\eta| < 2.5$



Dilepton resonances - Invariant mass spectra

Mass spectra divided into three regions:

$60 \text{ GeV} < M_{\ell\ell} < 120 \text{ GeV}$: Z peak

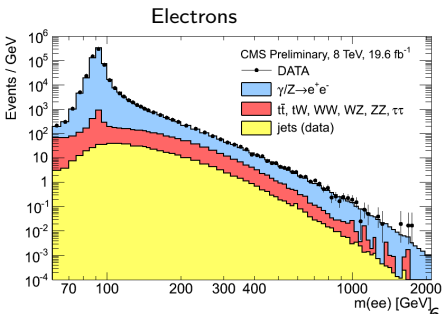
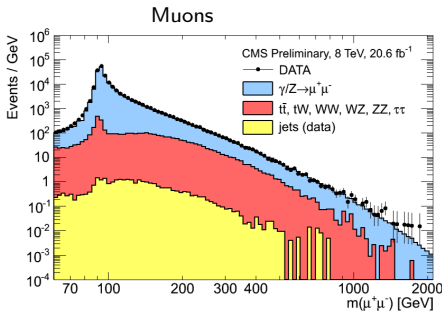
- Study lepton efficiencies and energy/momentum scales

$120 \text{ GeV} < M_{\ell\ell} < 200 \text{ GeV}$: Control region

- No new physics found at Tevatron
- Test agreement of data and expectation beyond the Z peak

$M_{\ell\ell} > 200 \text{ GeV}$: Signal region

Data well described by the expectation

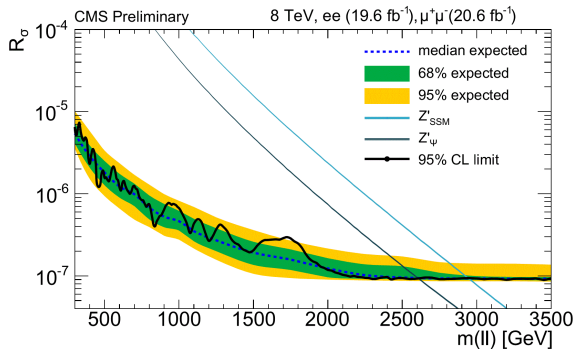


Dilepton resonances - Results

Bayesian 95% CL upper limits on Z'/Z cross section ratio, assuming narrow spin-1 resonance

$$R_\sigma = \frac{\sigma(pp \rightarrow Z' + X \rightarrow \ell^+\ell^- + X) [0.6 M_{Z'}, 1.4 M_{Z'}]}{\sigma(pp \rightarrow Z + X \rightarrow \ell^+\ell^- + X) [60 \text{ GeV}, 120 \text{ GeV}]}$$

Combination of dimuon and dielectron channels



Dominant syst. uncertainties

Ratio of $A \times \epsilon$ between Z' and Z :

3% for $\mu\mu$

4% for barrel-barrel ee

6% for barrel-endcap ee

Uncertainty on the background fit
PDFs and higher order corrections:

2% at $M_{\ell\ell} = 200 \text{ GeV}$

20% at $M_{\ell\ell} = 3 \text{ TeV}$

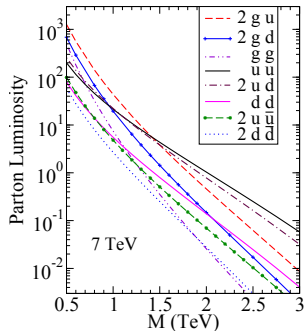
95% CL lower limits on Z' mass

Z'_SSM : $M_{Z'} > 2.96 \text{ TeV}$, Z'_ψ : $M_{Z'} > 2.60 \text{ TeV}$

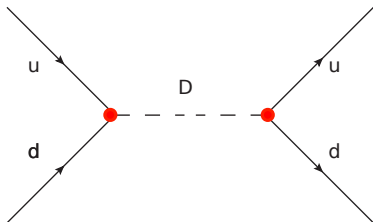
Dijet resonances - Signal models

Search for narrow dijet resonances CMS-PAS-EXO-12-059

Model Name	X	Color	J	Decay
String resonances	S	mixed	mixed	$qg, q\bar{q}, gg$
Strong couplings				
Excited quark	q^*	Triplet	1/2	qg
Axigluon	A	Octet	1	$q\bar{q}$
Coloron	C	Octet	1	$q\bar{q}$
s8 resonance	s8	Octet	0	gg
Weak couplings				
Heavy W	W'	Singlet	1	$q\bar{q}$
Heavy Z	Z'	Singlet	1	$q\bar{q}$
E_6 diquark	D	Triplet	0	qq
RS graviton	G	Singlet	2	$q\bar{q}, gg$



Plot taken from T. Han, I. Lewis, Z. Liu; JHEP12(2010)085



Signal description

Cross section

- Strongly vs. weakly coupled models
- Parton luminosity of initial state

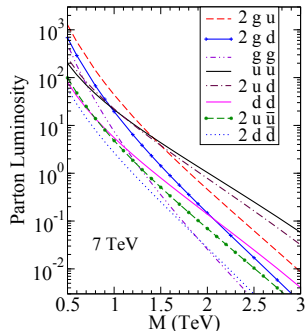
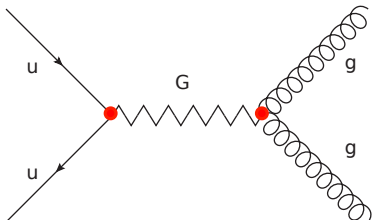
Resonance shape

- Impact of FSR depending on final state

Dijet resonances - Signal models

Search for narrow dijet resonances CMS-PAS-EXO-12-059

Model Name	X	Color	J	Decay
String resonances	S	mixed	mixed	$qg, q\bar{q}, gg$
Strong couplings				
Excited quark	q^*	Triplet	1/2	qg
Axigluon	A	Octet	1	$q\bar{q}$
Coloron	C	Octet	1	$q\bar{q}$
s8 resonance	s8	Octet	0	gg
Weak couplings				
Heavy W	W'	Singlet	1	$q\bar{q}$
Heavy Z	Z'	Singlet	1	$q\bar{q}$
E_6 diquark	D	Triplet	0	qq
RS graviton	G	Singlet	2	$q\bar{q}, gg$



Plot taken from T. Han, I. Lewis, Z. Liu; JHEP12(2010)085

Signal description

Cross section

- Strongly vs. weakly coupled models
- Parton luminosity of initial state

Resonance shape

- Impact of FSR depending on final state

Dijet reconstruction and resolution

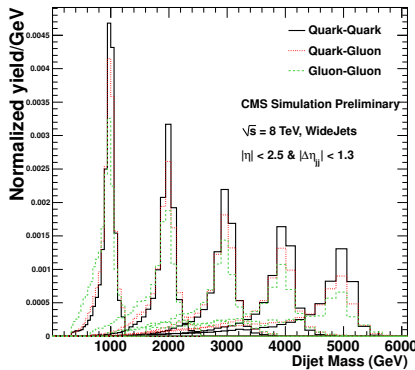
Standard jet reconstruction

- Particle-flow event reconstruction and jet identification
- Jets reconstructed with anti- k_T algorithm, jet parameter $R = 0.5$

Wide jet reconstruction

High jet energy → FSR significant
FSR recovery important for signal shape

- Select two leading jets
- Add other jets within $\Delta R < 1.1 = R_{wide}$
- R_{wide} determined in study of expected limits

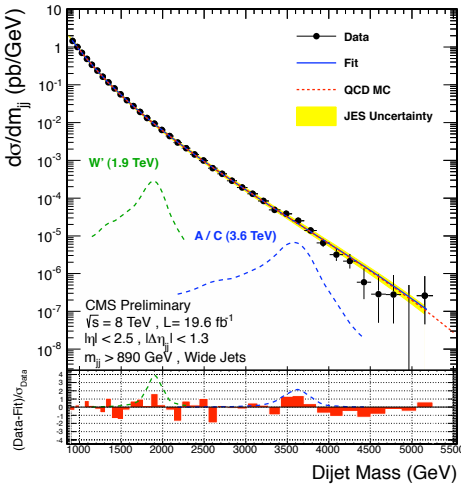
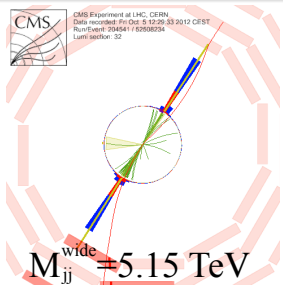


Effect of FSR stronger for gluon than quark jets
→ Statistical analysis for three signal shapes, depending on final state (qq , gq , gg)

Dijet resonances - Mass spectrum

Event selection

- $H_T > 650 \text{ GeV}$ OR $M_{jj}^{wide} > 750 \text{ GeV}$
- $p_T^{jet} > 30 \text{ GeV}$, $|\eta^{jet}| < 2.5$
- Wide jets built around two leading jets
- $|\Delta\eta_{jj}^{wide}| < 1.3$
- $M_{jj}^{wide} > 890 \text{ GeV}$

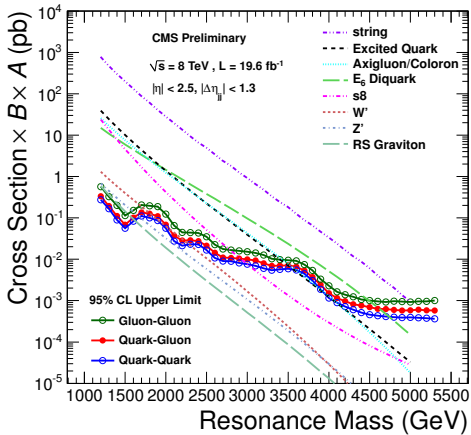


QCD background model from fit to data:

$$\frac{d\sigma}{dM} = P_0 \frac{\left(1 - M/\sqrt{s}\right)^{P_1}}{\left(M/\sqrt{s}\right)^{P_2 + P_3 \ln(M/\sqrt{s})}}$$

Dijet resonances - Results

Bayesian 95% CL upper cross section limits



Impact of signal shape

Limits on $\sigma \times BR \times A$ by factors 2 to 3
stronger for $q \bar{q}$ compared to gg final state

Dominant syst. uncertainties

Background

- Uncertainties on bkg fit parameters increase cross section limit by:

$\sim 100\%$ at $M = 1 \text{ TeV}$
 $\sim 20\%$ at $M = 2.5 \text{ TeV}$
 $< 5\%$ at $M > 3.5 \text{ TeV}$

Signal

- Jet energy scale: 1.3% shift of M_{res}

Limits - excerpts

Model	Mass Excl. [TeV]
String resonance	1.20-5.08
E_6 diquarks	1.20-4.75
Z'	1.20-1.68
RS graviton	1.20-1.58

Further dijet resonance results:
dijets with b-tag, CMS-PAS-EXO-12-023
dijets with W/Z-tag, arXiv:1405.1994

$\gamma + \text{jet resonances} - \text{Excited quarks}$

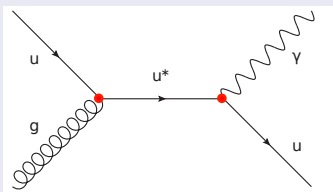
Quarks as composite objects \rightarrow excited quarks q^*

CMS-PAS-EXO-13-003

$$\mathcal{L}_{\text{transition}}^{q \leftrightarrow q^*} = \frac{1}{2\Lambda} \bar{q}_R^* \sigma^{\mu\nu} \left[g_s f_s \frac{\lambda_a}{2} G_{\mu\nu}^a + g f \frac{\tau}{2} W_{\mu\nu} + g' f' \frac{Y}{2} B_{\mu\nu} \right] q_L + \text{h.c.}$$

Excited quark model

- s-channel q^* production at the LHC:

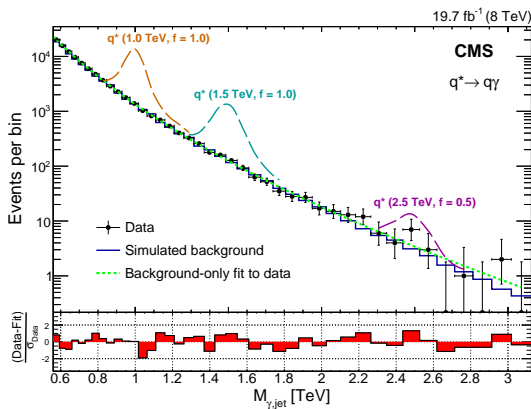


- Mass-degenerate, first generation excited quarks (u^*, d^*) considered
- Free parameters: compositeness scale Λ , M_{q^*} , three coupling strengths; assumption: $f = f_s = f'$

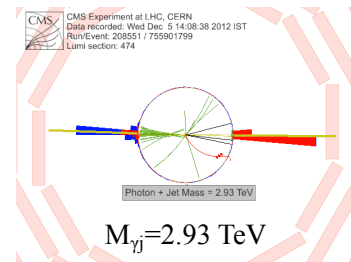
Event selection

- Single-photon trigger $E_T^\gamma > 150$ GeV
- Event reconstruction based on particle-flow algorithm
- $p_T^\gamma > 170$ GeV, $|\eta^\gamma| < 1.444$
- $p_T^{\text{jet}} > 170$ GeV, $|\eta^{\text{jet}}| < 3.0$
 $\Delta R(\gamma, \text{jet}) > 0.5$
- $|\Delta\eta(\gamma, \text{jet})| < 2.0$
 $|\Delta\phi(\gamma, \text{jet})| > 1.5$
- $M_{\gamma, \text{jet}} > 560$ GeV

$\gamma + \text{jet}$ resonances - Invariant mass $M_{\gamma\text{jet}}$



$M_{\gamma\text{jet}}$ core resolution
4.5% at 1 TeV, 3% at 3 TeV



Background composition

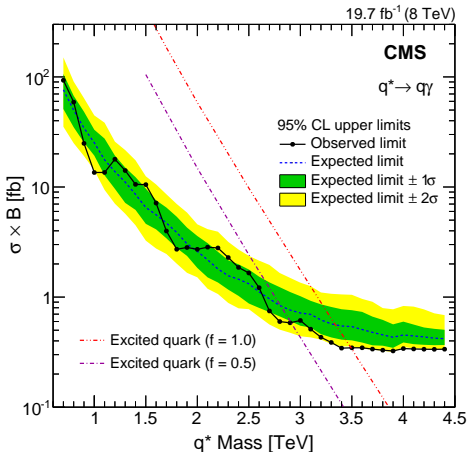
Background fit modelling mass dependence of background due to PDFs and QCD ME:

$$\frac{d\sigma}{dM} = P_0 \frac{\left(1 - M/\sqrt{s}\right)^{P_1}}{\left(M/\sqrt{s}\right)^{P_2 + P_3 \ln(M/\sqrt{s})}}$$

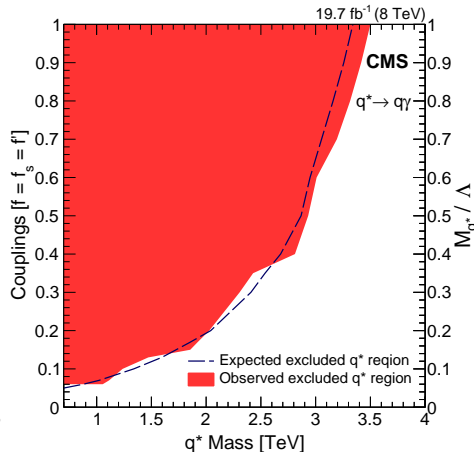
Process	Fraction
$q\bar{q} \rightarrow \gamma g$	80.5%
$qg \rightarrow \gamma q$	18.5%
QCD dijet	1%
$W/Z + \gamma$	1%

$\gamma + \text{jet}$ resonances - Results

Bayesian 95% CL cross section limits,
theory curves for $\Lambda = M_{q^*}$



Corresponding exclusion in
coupling vs M_{q^*} parameter space



Exclusion range for $f = 1.0 : 0.7 \text{ TeV} - 3.5 \text{ TeV}$

Dileptons - Anticipating higher \sqrt{s}

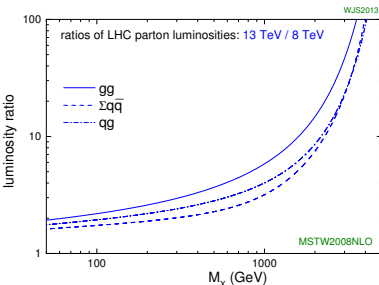
Short term projection for 2015

Expect to extend current discovery reach early in the planned $\sqrt{s} = 13$ TeV run!

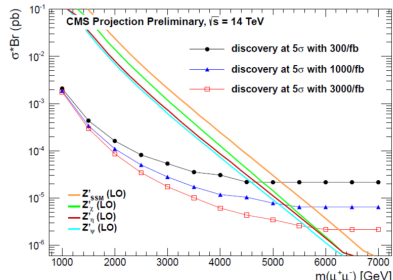
Long term projections

- Discovery reach at $\sqrt{s} = 14$ TeV studied with integrated luminosities of 300 fb^{-1} , 1000 fb^{-1} , 3000 fb^{-1}
- Generator level events smeared to the detector response
- $A \cdot \epsilon$ and resolution from $\sqrt{s} = 8$ TeV analysis

Expect sensitivity to Z' 's with $M_{Z'} \gtrsim 5$ TeV



W.J. Stirling, private communication



CMS-NOTE-2013-002; arXiv:1307.7135

Summary

High-mass resonance searches at CMS up to now

- No new physics observed in high-mass ($M \gg 125$ GeV) resonance searches at CMS, yet
- Wide range of theories of physics beyond the SM probed and new limits set
- Exclusion limits pushed into the multi-TeV range, for example:
 - Dileptons: Z'_{SSM} : $M_{Z'} > 2.96$ TeV
 - Dijets: E_6 diquarks: $M_D > 4.75$ TeV
 - $\gamma +$ jet: Excited quarks: $M_{q^*} > 3.5$ TeV

Summary

High-mass resonance searches at CMS up to now

- No new physics observed in high-mass ($M \gg 125$ GeV) resonance searches at CMS, yet
- Wide range of theories of physics beyond the SM probed and new limits set
- Exclusion limits pushed into the multi-TeV range, for example:
 - Dileptons: Z'_{SSM} : $M_{Z'} > 2.96$ TeV
 - Dijets: E_6 diquarks: $M_D > 4.75$ TeV
 - $\gamma +$ jet: Excited quarks: $M_{q^*} > 3.5$ TeV

Summary

High-mass resonance searches at CMS up to now

- No new physics observed in high-mass ($M \gg 125$ GeV) resonance searches at CMS, yet
- Wide range of theories of physics beyond the SM probed and new limits set
- Exclusion limits pushed into the multi-TeV range, for example:
 - Dileptons: Z'_{SSM} : $M_{Z'} > 2.96$ TeV
 - Dijets: E_6 diquarks: $M_D > 4.75$ TeV
 - $\gamma + \text{jet}$: Excited quarks: $M_{q^*} > 3.5$ TeV

Summary

High-mass resonance searches at CMS up to now

- No new physics observed in high-mass ($M \gg 125$ GeV) resonance searches at CMS, yet
- Wide range of theories of physics beyond the SM probed and new limits set
- Exclusion limits pushed into the multi-TeV range, for example:

Dileptons: Z'_{SSM} : $M_{Z'} > 2.96$ TeV

Dijets: E_6 diquarks: $M_D > 4.75$ TeV

$\gamma +$ jet: Excited quarks: $M_{q^*} > 3.5$ TeV

Looking forward to (early) 2015 and beyond

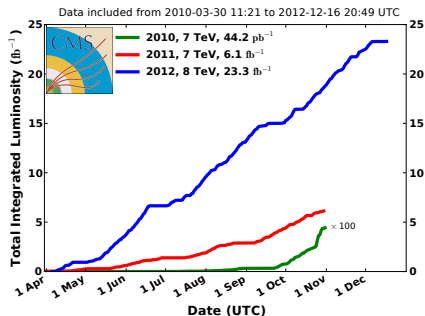
- Resonance searches at high mass gain significantly from increase in center-of-mass energy
- Looking forward to first fb^{-1} of $\sqrt{s} = 13$ TeV data

Backup slides

LHC & CMS performance

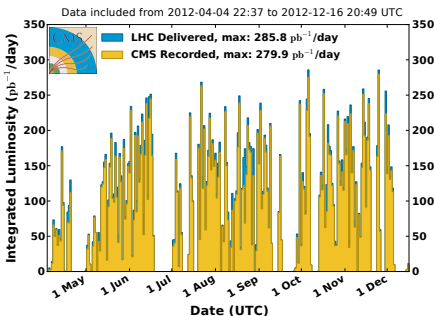
Cumulative pp luminosity delivered

CMS Integrated Luminosity, pp



93.5% of delivered luminosity recorded

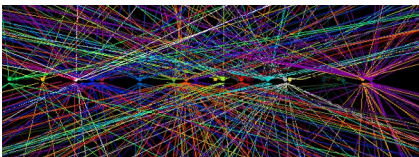
CMS Integrated Luminosity Per Day, pp , 2012, $\sqrt{s} = 8 \text{ TeV}$



Analyzed datasets

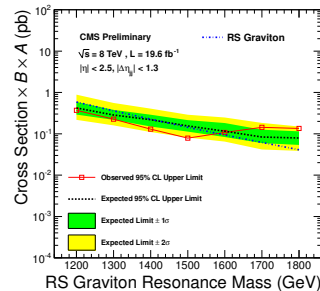
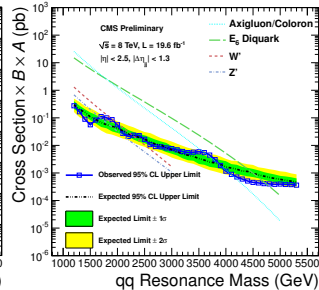
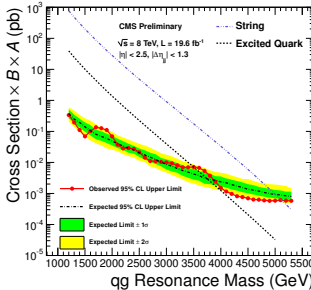
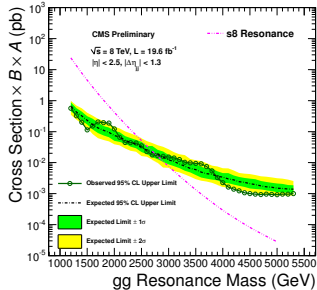
- Analyses based on $\sqrt{s} = 8 \text{ TeV}$ data
- Subdetector requirements reduce analyzed integrated luminosity to:

dimuon analysis: $L_{int} = 20.6 \text{ fb}^{-1}$
other analyses shown: $L_{int} = 19.6 \text{ fb}^{-1}$



Luminosity up to 7.67 Hz/nb at 50 ns bunch spacing
→ On average 21 interactions per bunch crossing

Dijet resonances - Results overview



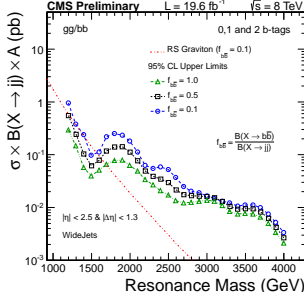
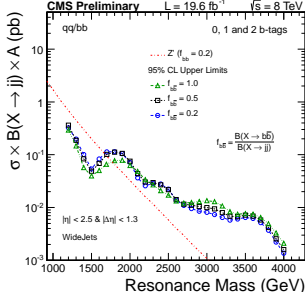
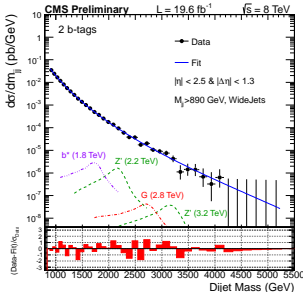
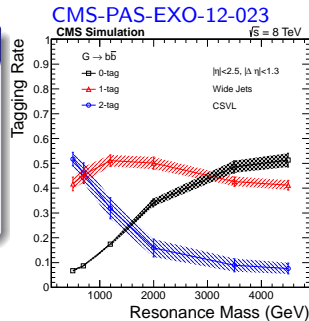
Model	Final State	Obs. Mass Excl. [TeV]	Exp. Mass Excl. [TeV]
String Resonance (S)	qg	[1.20, 5.08]	[1.20, 5.00]
Excited Quark (q^*)	qg	[1.20, 3.50]	[1.20, 3.75]
E_6 Diquark (D)	qq	[1.20, 4.75]	[1.20, 4.50]
Axigluon (A)/Coloron (C)	q \bar{q}	[1.20, 3.60] + [3.90, 4.08]	[1.20, 3.87]
Color Octet Scalar (s8)	gg	[1.20, 2.79]	[1.20, 2.74]
W' Boson (W')	q \bar{q}	[1.20, 2.29]	[1.20, 2.28]
Z' Boson (Z')	q \bar{q}	[1.20, 1.68]	[1.20, 1.87]
RS Graviton (G)	q \bar{q} +gg	[1.20, 1.58]	[1.20, 1.43]

Dijet resonances - b-tagged jets

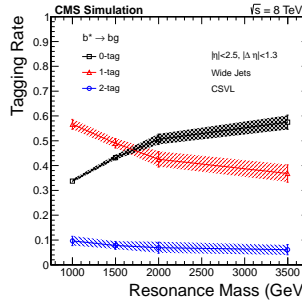
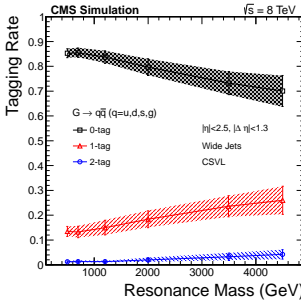
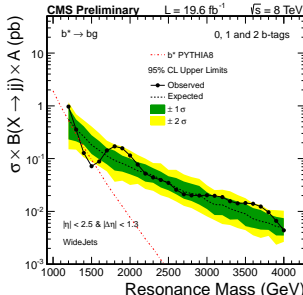
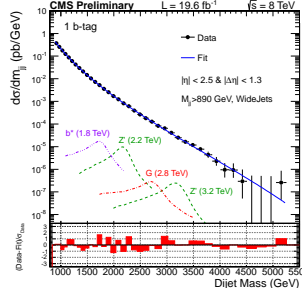
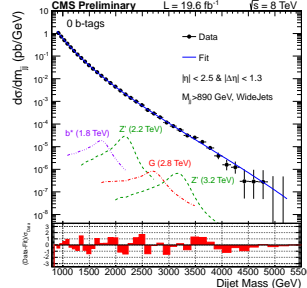
Extension of dijet search: b-tagging

- Selected dijet events split into 0,1,2 b-tag categories
- Parameter added to signal model: $f_{b\bar{b}} = \frac{BR(X \rightarrow b\bar{b})}{BR(X \rightarrow jj)}$
- Three signal types: gg/bb (RS), $q\bar{q}/bb$ (Z'), bg (b^*)
- Signal shapes per category depending on $f_{b\bar{b}}$, $\epsilon_{b\text{-tag}}$

Process	$Z' f_{b\bar{b}} = 0.2$	$RS f_{b\bar{b}} = 0.1$	$b^* \rightarrow bg$
Exclusion 95% CL [TeV]	1.20 – 1.68	1.42 – 1.57	1.34 – 1.54



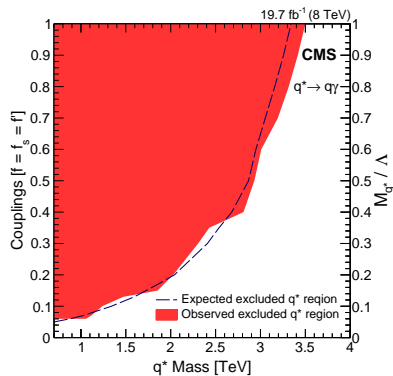
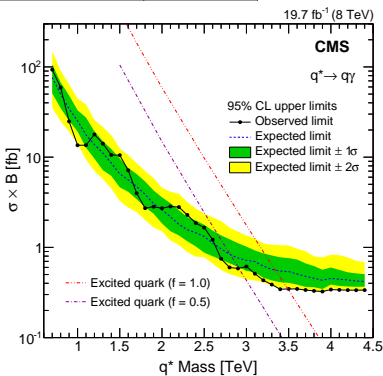
Dijet resonances - b-tagged jets II



$\gamma + \text{jet}$ resonances - Results

	$\sigma_{\text{syst}} [\%]$
jet energy res.	10
jet energy scale	1.0-1.4
γ energy res.	0.5
γ energy scale	1.5
L_{int}	2.6
$A \cdot \epsilon$ (signal)	4
$\mu_{\text{ren}}, \mu_{\text{fac}}$	4

- **Energy resolution uncertainties:**
5% uncertainty on $M_{\gamma\text{jet}}$ resolution
- **Energy scale uncertainties:** 1% shift of resonance mass
- **Stat. uncertainty bkg fit:** 1% at 1 TeV, 30% at 3 TeV
- **FSR scale variation:**
7% (1 TeV) , 4% (3 TeV) change in resonance width



Exclusion range for $f = 1.0$: 0.7 TeV – 3.5 TeV

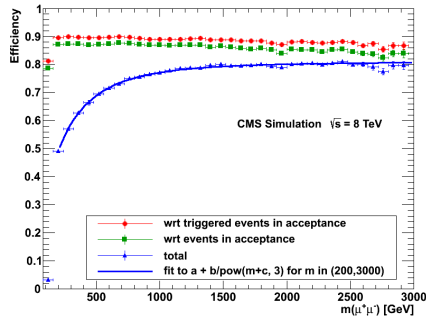
$\gamma + \text{jet}$ resonances - Signal efficiencies

Selection	1 TeV (%)	4 TeV (%)
Photon ID	70.2	70.9
$p_T^\gamma > 170 \text{ GeV}$	67.2	70.4
$ \eta^\gamma < 1.4442$	65.0	68.2
$p_T^{\text{jet}} > 170 \text{ GeV}$	63.6	68.1
$ \eta^{\text{jet}} < 3.0$	63.4	68.1
$\Delta\phi(\gamma, \text{jet}) > 1.5$	63.3	68.0
$ \Delta\eta(\gamma, \text{jet}) < 2.0$	54.6	57.4
$M_{\gamma, \text{jet}} > 560 \text{ GeV}$	54.2	57.3

Event selection: Muons

Muon selection

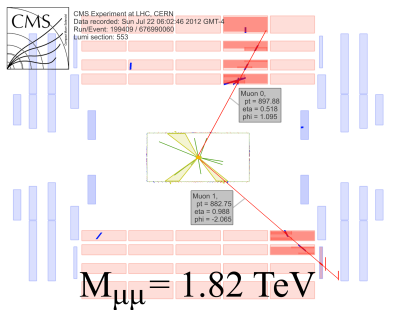
- Reconstructed in inner tracker and muon system, cuts on track quality
- Relative uncertainty on p_T^μ , $\frac{\delta p_T^\mu}{p_T^\mu} < 0.3$
- Isolation based on tracker information



Dimuon event selection

Single-muon trigger, $p_T^\mu > 40$ GeV, $|\eta^\mu| < 2.1$

- Two muons with $p_T^\mu > 45$ GeV, $|\eta^\mu| < 2.4$
- Muon tracks from the same vertex
- Muons carry opposite electric charge
- Cut on dimuon opening angle against muons from cosmic rays



Event selection: Electrons

Electron selection

- ECAL cluster satisfying shower shape criteria
- Small relative energy deposit in HCAL behind the ECAL cluster
- Isolation in both ECAL and HCAL
- ECAL cluster matched to isolated track
- Cuts to reject converted photons
- E_T assignment based on ECAL cluster

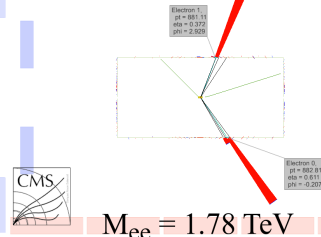
Dielectron event selection

Double-electron trigger, $E_T > 33$ GeV

- Two selected electrons with $E_T > 35$ GeV
- Analysis split into two channels
 - Both electrons in barrel $|\eta| < 1.422$
 - One electron in barrel and one in endcap $1.560 < |\eta| < 2.5$

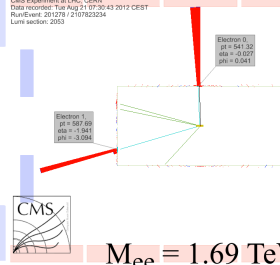
Both electrons in the barrel

CMS Experiment at LHC, CERN
Data recorded: Sun Jul 15 03:34:01 2012 CEST
RunEvent: 198869 / 1188478742
Lumi section: 1021



One electron in the barrel, one in the endcap

CMS Experiment at LHC, CERN
Data recorded: Tue Aug 21 07:30:43 2012 CEST
RunEvent: 201028 / 2107823234
Lumi section: 2053

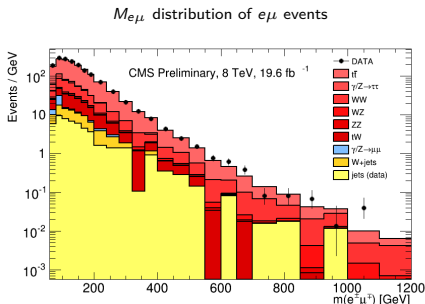


Background expectation

Three different types of background:

Irreducible Z/γ^* background

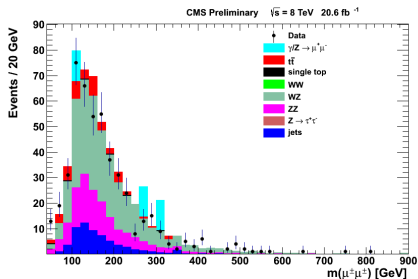
- **Largest background:** $\sim 75\%$ (ee), 80% ($\mu\mu$) of expected events above $M_{\ell\ell} = 200$ GeV
- Shape from simulation (POWHEG)
- Higher-order corrections studied with FEWZ (NNLO QCD) and HORACE (NLO EWK)



$t\bar{t}$, tW , diboson backgrounds

- $\sim 20\%$ above $M_{\ell\ell} = 200$ GeV
- Flavor symmetric \rightarrow Examine $e\mu$ spectrum in data to cross-check simulation

$M_{\mu\mu}$ of dimuon events with same-sign charge combination



Jets misidentified as leptons

- W +jet, QCD multijet, γ +jet
- Negligible for muon channel
- Derived from data

Invariant mass spectra

Mass spectra divided into three regions:

60 GeV < $M_{\ell\ell}$ < 120 GeV: Z peak

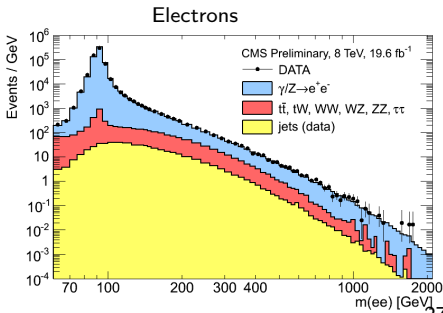
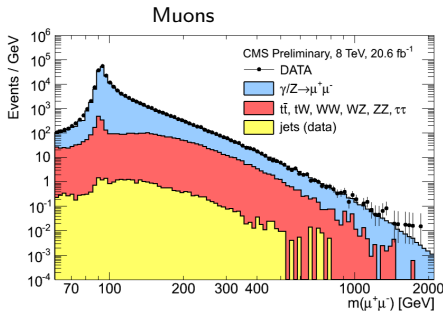
- Normalization of the simulated background
- Measurement of reconstruction, ID and trigger efficiencies up to $p_T^\mu, E_T^e \sim 300$ GeV
- Study of electron energy/muon momentum scale and resolution

120 GeV < $M_{\ell\ell}$ < 200 GeV: Control region

- No new physics expected (Tevatron)
- Test agreement of data and expectation beyond the Z peak

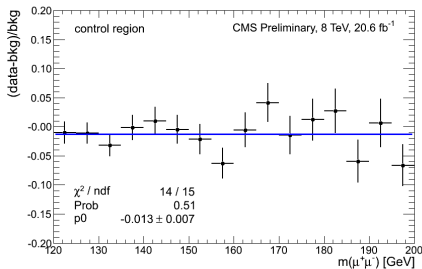
$M_{\ell\ell} > 200$ GeV: Signal region

Data well described by the expectation

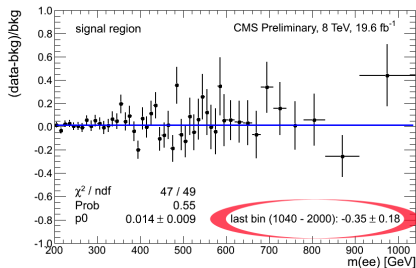
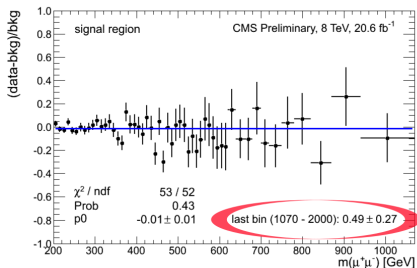
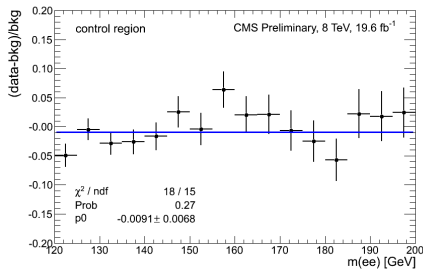


Invariant mass spectra - data/expectation ratio plots

Muons



Electrons



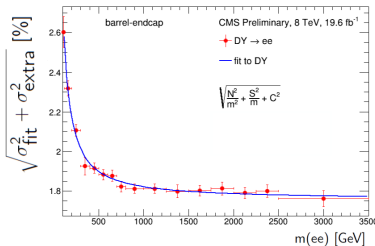
Plots show statistical uncertainties, only. No excess observed, setting limits.

Model and limit setting

Model & signal region

- Signal model:
 $BW(M_{\ell\ell}|M_{Z'}, \Gamma_{Z'}) \otimes \text{Gauss}(M_{\ell\ell}|\sigma_{resolution})$
- Background model: Parameterized function, shape from fit to simulation
- Data considered: Events with $M_{\ell\ell} > 200$ GeV
- Mass window: $M_{Z'} \pm 6$ times mass resolution

Relative invariant mass resolution
(electron barrel-endcap)



Limit setting

Bayesian 95% CL upper limits on Z' to Z cross section ratio R_σ

$$R_\sigma = \frac{\sigma(pp \rightarrow Z' + X \rightarrow \ell^+\ell^- + X)}{\sigma(pp \rightarrow Z + X \rightarrow \ell^+\ell^- + X)} = \frac{N(Z' \rightarrow \ell^+\ell^-)}{N(Z \rightarrow \ell^+\ell^-)} \cdot \frac{A(Z \rightarrow \ell^+\ell^-)}{A(Z' \rightarrow \ell^+\ell^-)} \cdot \frac{\epsilon(Z \rightarrow \ell^+\ell^-)}{\epsilon(Z' \rightarrow \ell^+\ell^-)}$$

$\sigma(Z')$ evaluated in mass range $M_{Z'} \pm 40\%$, $\sigma(Z)$ evaluated in 60 GeV $< M_{\ell\ell} < 120$ GeV

- Uncertainty on the luminosity cancels in the ratio R_σ
- Uncertainties on the absolute values of $\epsilon_{\text{trigger}}$, $\epsilon_{\text{reconstruction}}$ and mass scale reduce to uncertainties on their evolution from the Z peak to high mass

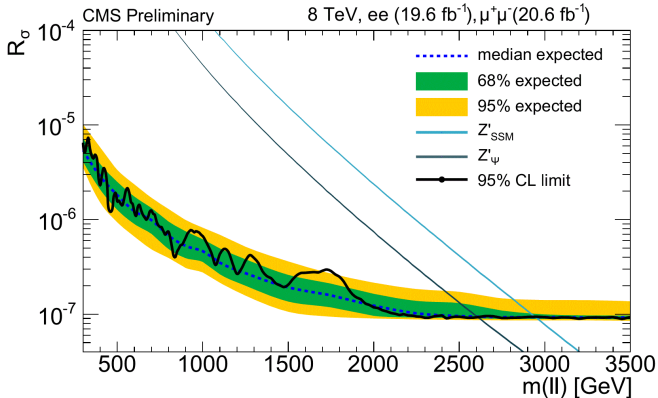
Systematic uncertainties

Systematic uncertainties

- Dominant uncertainty on the limits:
Ratio of acceptance times efficiency between Z' and Z
3% for dimuon, 4% for barrel-barrel and 6% for barrel-endcap dielectron channel
- Z/γ^* background:
Shape uncertainty on the background fit from PDFs and higher order corrections
ranges from 2% at $M_{\ell\ell} = 200$ GeV to 20% at $M_{\ell\ell} = 3000$ GeV
- Uncertainties on the subleading backgrounds studied but less important
- Impact of uncertainty on the muon momentum scale studied with different detector misalignment scenarios and found to be negligible

Limits

Bayesian 95% CL upper limits on R_σ , assuming narrow spin-1 resonance
Limits for combination of dimuon and dielectron channels



Signal cross sections for Z'_SSM and Z'_ψ scaled to NNLO QCD

95% CL lower limits on Z' mass

Z'_SSM : $M_{Z'} > 2.96 \text{ TeV}$, Z'_ψ : $M_{Z'} > 2.60 \text{ TeV}$

Dileptons - Projection for $\sqrt{s} = 14$ TeV

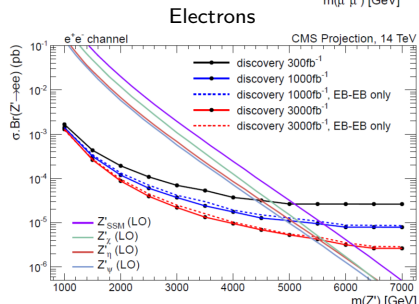
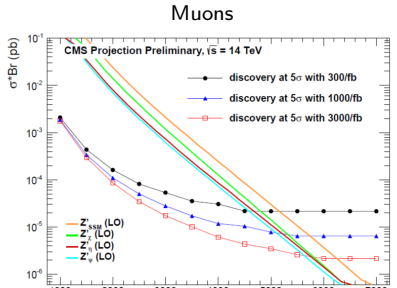
Long term projections

- Discovery reach at $\sqrt{s} = 14$ TeV studied with integrated luminosities of 300 fb^{-1} , 1000 fb^{-1} , 3000 fb^{-1}
- Generator level events smeared to the detector response
- $A \cdot \epsilon$ and resolution from $\sqrt{s} = 8$ TeV analysis

Expect sensitivity to Z' 's with $M_{Z'} \gtrsim 5$ TeV

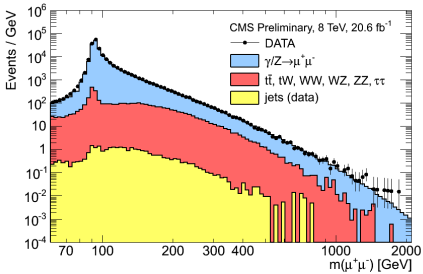
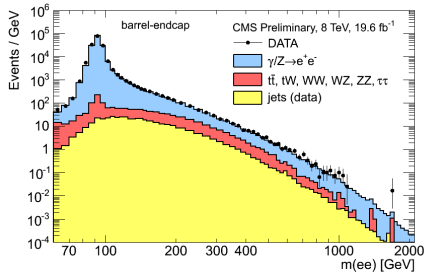
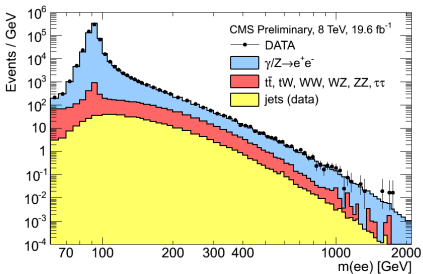
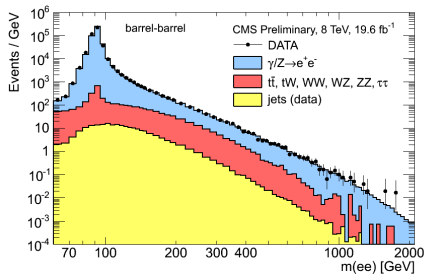
Short term projection for 2015

Expect to extend current discovery reach early in the planned $\sqrt{s} = 13$ TeV run!

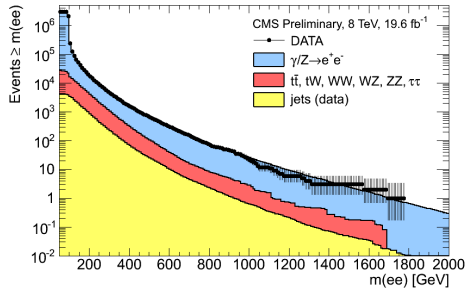
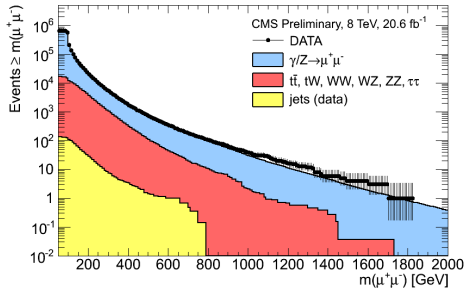


Reference: CMS-NOTE-2013-002; arXiv:1307.7135

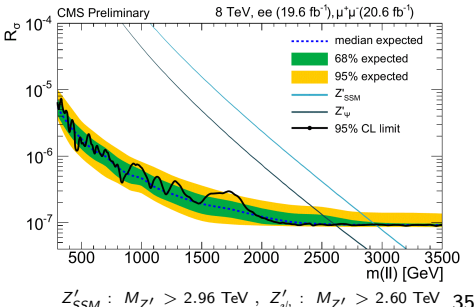
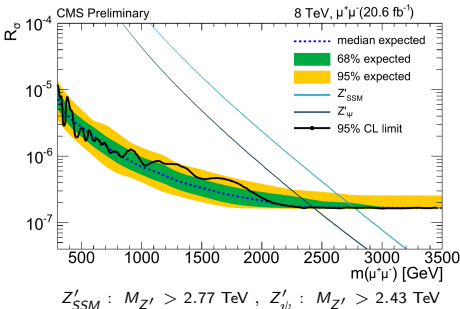
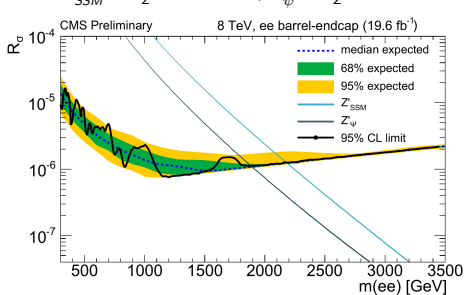
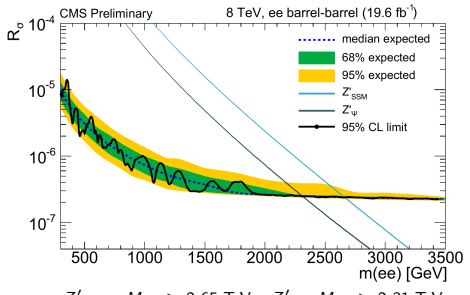
Invariant mass spectra - all channels



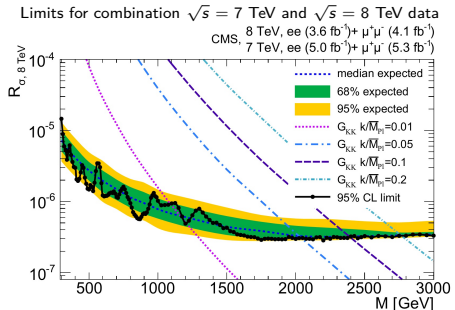
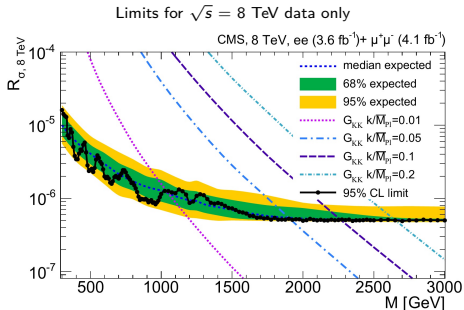
Invariant mass spectra - cumulative distributions



Limits - all channels



Limits on spin-2 resonance (RS graviton)



- Spin-2 resonance
- Couplings to $q\bar{q}$ and $gg \rightarrow$ different acceptance compared to Z'_{SSM} and Z'_{ψ}
- Combination of $\sqrt{s} = 7$ TeV and $\sqrt{s} = 8$ TeV datasets only valid for models with the same $q\bar{q}$ to gg coupling ratio as RS graviton

Lower mass limits

$\sqrt{s} = 8$ TeV data only:

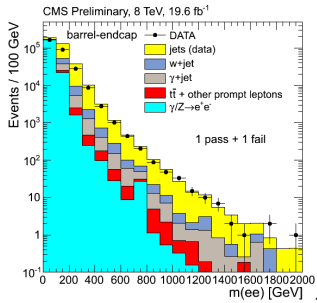
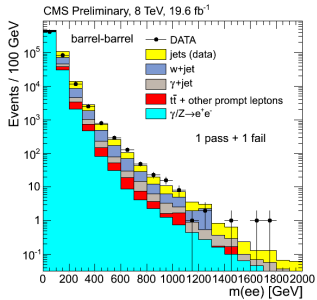
- $G_{KK}(k/\bar{M}_{Pl} = 0.1)$: 2260 GeV
- $G_{KK}(k/\bar{M}_{Pl} = 0.05)$: 1900 GeV

$\sqrt{s} = 7$ TeV and $\sqrt{s} = 8$ TeV data:

- $G_{KK}(k/\bar{M}_{Pl} = 0.1)$: 2390 GeV
- $G_{KK}(k/\bar{M}_{Pl} = 0.05)$: 2030 GeV

Background from jets misidentified as electrons

- Measure rate of jets identified as electron candidates with a 'loose' electron ID passing the electron ID used in the analysis
 - Select jet enriched control sample using single photon triggers and asking for a single 'loose' electron candidate
 - Subtract contamination from processes with real electrons from simulation
 - Determine so-called 'fake-rate' FR
- Apply the measured 'fake-rate'
 - Multijet contribution:
Select multijet background enriched control sample with two 'loose' electron candidates that fail the electron ID used in the analysis
Weight each electron by $FR/(1 - FR)$
 - For further contributions ($W + \text{jet}$, $\gamma + \text{jet}$) apply measured 'fake-rate' to simulation
- 40% systematic uncertainty applied

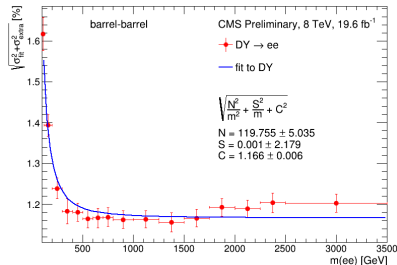


Invariant mass resolution

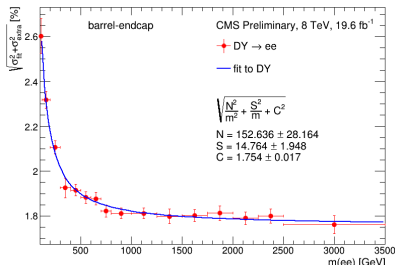
Dielectron channels:

- Fit double-sided Crystal Ball function convoluted with Breit Wigner function to $M_{\ell\ell}^{\text{reco}} - M_{\ell\ell}^{\text{true},MC}$ in simulated Drell-Yan samples in different mass bins
- Invariant mass resolution from simulation corrected for difference between resolutions at the Z peak obtained from data and simulation

Resolution in barrel-barrel channel



Resolution in barrel-endcap channel

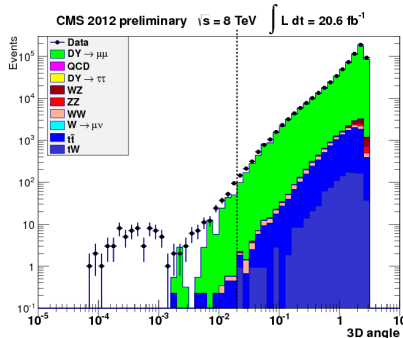


Dimuon channel:

- Invariant mass resolution obtained from Gaussian fits to $(M_{\ell\ell}^{\text{reco}} - M_{\ell\ell}^{\text{true},MC}) / M_{\ell\ell}^{\text{true},MC}$ in simulated Drell-Yan samples
- Different detector misalignment scenarios consistent with alignment studies compared
- Invariant mass resolution in the dimuon channel is $\sim 4\%$ at $M_{\mu\mu} = 1$ TeV and $\sim 9\%$ at $M_{\mu\mu} = 3$ TeV

Background from muons from cosmic rays

Opening angle between the two muons required to be smaller than $\pi - 0.02$ rad
Plotted: $\alpha = \pi - \text{opening angle}$

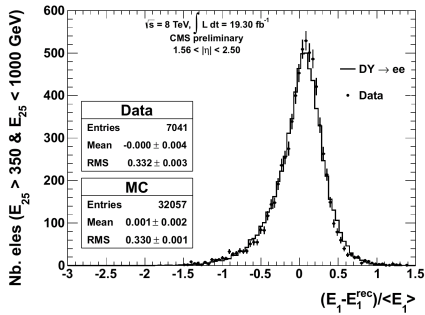


Both the cut on α and the primary vertex requirement have been removed in this plot
The already small contribution from cosmic muons lies mainly in the region $\alpha < 0.002$

ECAL response at high electron energy

- Single ECAL crystal readout electronics saturate at high energies (~ 1.7 TeV in the barrel, ~ 3.0 TeV in the endcaps)
- Linearity of ECAL energy response at high energies tested by relating the energy deposit in the single crystal with the highest energy deposit (E_1) to the energy deposits in the 24 surrounding crystals in a 5×5 crystal matrix (E_{25})
- Algorithm describing this relation takes into account the impact point position on the crystal face
- Parameters of the algorithm taken from simulation
- Measured energy deposit E_1 compared to E_1^{rec} determined from the 24 surrounding crystals

Electrons with $E_{25} > 350$ GeV in the endcaps



Electrons with $E_{25} > 350$ GeV in the barrel

